

Testing Modified Dark Matter with Galaxy Clusters

Does Dark Matter know about the Cosmological Constant?

Doug Edmonds,^{1,2*} Duncan Farrah,^{2*} Chiu Man Ho,^{3*}
Djordje Minic,^{2,4*} Y. Jack Ng,^{5*} and Tatsu Takeuchi^{2,4*}

¹ *Department of Physics, Emory & Henry College, Emory, VA 24327, USA*

² *Department of Physics, Virginia Tech, Blacksburg, VA 24061, USA*

³ *Department of Physics and Astronomy, Michigan State University, East Lansing, MI 48824, USA*

⁴ *Center for Neutrino Physics, Department of Physics, Virginia Tech, Blacksburg, VA 24061, USA*

⁵ *Institute of Field Physics, Department of Physics and Astronomy, University of North Carolina, Chapel Hill, NC 27599, USA*

Accepted XXX. Received YYY; in original form ZZZ

ABSTRACT

We discuss the possibility that the cold dark matter mass profiles contain information on the cosmological constant Λ , and that such information constrains the nature of cold dark matter (CDM). We call this approach Modified Dark Matter (MDM). In particular, we examine the ability of MDM to explain the observed mass profiles of 13 galaxy clusters. Using general arguments from gravitational thermodynamics, we provide a theoretical justification for our MDM mass profile and successfully compare it to the NFW mass profiles both on cluster and galactic scales. Our results suggest that indeed the CDM mass profiles contain information about the cosmological constant in a non-trivial way.

Key words: dark matter, galaxies: clusters: general

1 INTRODUCTION

1.1 Evidence for Dark Matter

Observational evidence for the presence of dark matter (Zwicky 1933, 1937) exists at a variety of length scales. It is most obvious at galactic scales (~ 10 kpc) where the rotation curves of spiral galaxies have been found to be asymptotically flat, way beyond the radii of their visible disks (Rubin & Ford 1970; Rubin, Ford & Thonnard 1978, 1980; van Albada et al. 1985). Measurements of rotation curves have also been performed for elliptical (Ciardullo, Jacoby & Djonghe 1993; Norris et al. 2012) and low-surface-brightness (LSB) galaxies (de Blok & Bosma 2002) with similar discrepancies. The dark matter to baryonic matter ratio inferred from the rotation curves differs from galaxy to galaxy. Extreme cases such as galaxies whose rotation curves do not require dark mat-

ter (Ciardullo, Jacoby & Djonghe 1993; Romanowsky et al. 2003) have also been discovered.^{1, 2}

At the scale of galaxy clusters (~ 1 Mpc), the virial theorem is used (assuming virialization of the galaxies and gas within the cluster) to infer the mass distribution within the cluster from the distribution of the radial velocities of member galaxies (Zwicky 1933, 1937), and the temperature and density distributions of the hot gases (the intracluster medium (ICM)) measured by X-ray satellite observatories (Sarazin 1988; Vikhlinin et al. 2005, 2006; Moretti et al. 2011). Strong and weak gravitational lensing also provide independent measurements of the cluster’s mass (Clowe, Gonzalez & Markevitch 2004). These determinations of the dynamical masses of the galaxy clusters dis-

¹ This does not mean that dark matter halos are ruled out in these galaxies. For example, in De Lorenzi et al. (2008), it is shown that a dark matter halo is consistent with observations of NGC 4697 though a halo is not required to fit the data.

² In the case of Globular clusters, which have radii on the scale of ~ 10 pc, there seems to be some controversy on whether they have a significant dark matter component (Mashchenko & Sills 2005a,b; Conroy, Loeb & Spergel 2011). A recent paper claims to have discovered globular clusters dominated by dark matter (Taylor et al. 2015).

* e-mails: dedmonds@ehc.edu, farrah@vt.edu, cmho@msu.edu, dminic@vt.edu, yjng@physics.unc.edu, takeuchi@vt.edu

agree with their visible masses, giving rise to the so-called virial discrepancy.

At the cosmological scale (~ 10 Gpc), the amount of dark matter in the universe can be inferred from the positions and heights of the acoustic peaks in the Cosmic Microwave Background (CMB) anisotropy data (Ade et al. 2015).

1.2 CDM & MOND

The most popular model which is consistent with various cosmological structure formation constraints is the one in which a non-zero cosmological constant Λ (dark energy) is assumed in addition to the existence of collisionless Cold Dark Matter (CDM) (Bertone, Hooper & Silk 2005; Frenk & White 2012). However, the Λ CDM paradigm is not without its problems at and below the galactic scale. In particular, N -body simulations of CDM evolution (Dubinski & Carlberg 1991; Navarro, Frenk & White 1996, 1997; Moore et al. 1999; Klypin et al. 2001; Taylor & Navarro 2001; Colín et al. 2004; Diemand et al. 2005) predict a ‘cusp’ in the dark matter distribution toward the galactic center whereas observations indicate the presence of a ‘core,’ i.e. the ‘core/cusp problem’ (de Blok 2010).

An alternative to the introduction of dark matter to explain the discrepancy between the visible and inferred masses would be to modify the laws of gravity. The most prominent of such approaches is Modified Newtonian Dynamics (MOND) of Milgrom (1983a,b,c).³ In MOND, the equation of motion is modified from $F = ma$ to

$$F = \begin{cases} ma & (a \gg a_c) \\ ma^2/a_c & (a \ll a_c) \end{cases} \quad (1)$$

where a_c is the critical acceleration⁴ which separates the two regions of behavior. The two regions are connected by an interpolating function

$$F = ma \mu(a/a_c), \quad (2)$$

where

$$\mu(x) = \begin{cases} 1 & (x \gg 1) \\ x & (x \ll 1) \end{cases} \quad (3)$$

The choice of interpolating functions $\mu(x)$ is arbitrary, and an often used functional form is

$$\mu(x) = \frac{x}{(1+x^n)^{1/n}}, \quad n \in \mathbb{N}. \quad (4)$$

For a given (baryonic) source mass M , its gravitational attraction on a test mass m is $F = m(GM/r^2) \equiv ma_N$, where $a_N = GM/r^2$ is the usual Newtonian acceleration without

³ Other approaches to modifying gravity instead of introducing dark matter include the relativistic version of MOND by Bekenstein (2004), and Blanchet & Le Tiec (2008, 2009); Blanchet & Novak (2011); Berezhiani & Khoury (2015); Mannheim & O’Brien (2013); Moffat & Rahvar (2014).

⁴ In the MOND literature, the critical acceleration is usually denoted a_0 .

dark matter. Then the above modification to the equation of motion implies

$$a = \begin{cases} a_N & (a \gg a_c) \\ \sqrt{a_c a_N} & (a \ll a_c) \end{cases} \quad (5)$$

On the outskirts of galaxies, this implies

$$v^2 = ra \xrightarrow{r \rightarrow \infty} r\sqrt{a_c a_N} = \sqrt{a_c GM} \equiv v_\infty^2, \quad (6)$$

leading to flat rotation curves⁵ as well as the Baryonic Tully-Fisher relation (Tully & Fisher 1977; Steinmetz & Navarro 1999; McGaugh et al. 2000; Torres-Flores et al. 2011; McGaugh 2012)

$$M \propto v^4. \quad (7)$$

The most amazing thing about the MOND approach is that it succeeds in fitting the rotation curves of a large set of galaxies with the single universal parameter a_c which is consistently found to be (Begeman et al. 1991)

$$a_c \approx 10^{-8} \text{ cm/s}^2. \quad (8)$$

Other studies of MOND in the context of rotation curves include Sanders (1996); Sanders & Verheijen (1998); van den Bosch & Dalcanton (2000); Swaters, Sanders & McGaugh (2010). Given that the Hubble parameter is

$$\begin{aligned} H_0 &= (67.74 \pm 0.46) \text{ km/s/Mpc} \\ &= [(6.581 \pm 0.045) \times 10^{-8} \text{ cm/s}^2] / c, \end{aligned} \quad (9)$$

(see Table 4 of Ade et al. 2015) it has been noted that

$$a_c \approx \frac{cH_0}{2\pi}, \quad (10)$$

suggesting that MOND may have cosmological origins (Milgrom 1999).

The application of MOND to galaxy clusters has been less successful. Sanders (1999, 2003) shows that assuming the value of a_c found from galactic rotation curves, fitting MOND to galaxy clusters does reduce the virial discrepancy, but not sufficiently so, mainly due to large portions of the clusters remaining in the $a \gtrsim a_c$ regime. MOND also has difficulty explaining the weak gravitational lensing of the bullet cluster (Clowe, Gonzalez & Markevitch 2004). Thus, even with MOND, the introduction of dark matter may be unavoidable at cluster scales, which negates the original motivation for MOND.

1.3 Modified Dark Matter?

If one is to stay within the dark matter paradigm, the uncanny success of MOND at galactic scales, where collisionless CDM has problems, makes one ponder whether it would be possible to combine the salient features of MOND and CDM into a new framework of dark matter.

From the relativistic point of view, the choice between

⁵ In reality, rotation curves are not all flat, they display a variety of properties. See, e.g. Persic & Salucci (1991); Persic, Salucci & Stel (1996); Catinella, Giovanelli & Haynes (2006).

the introduction of dark matter and the modification of gravity amounts to which side of Einstein's equation,

$$G_{\alpha\beta} = (8\pi G)T_{\alpha\beta} , \quad (11)$$

one chooses to modify. The same terms could be interpreted differently depending on which side of the equation one places it, e.g. vacuum energy vs. cosmological constant. Thus if a particular modification works on the left-hand-side (a relativistic extension of MOND, for example), one could move it to the right-hand-side and reinterpret it as due to a new type of dark matter. This is also evident in the non-relativistic MOND equation, Eq. (2), when rewritten as

$$\frac{1}{\mu(a/a_c)} \frac{GM}{r^2} = a . \quad (12)$$

Interpreting M as the mass of baryonic matter enclosed within a sphere of radius r , one could write the left-hand-side as

$$\frac{1}{\mu(a/a_c)} \frac{GM}{r^2} = \frac{G(M + M')}{r^2} , \quad (13)$$

and interpret

$$M' = M \left[\frac{1}{\mu(a/a_c)} - 1 \right] \equiv M f_{\text{MOND}}(a/a_c) , \quad (14)$$

as the mass of non-baryonic dark matter enclosed within the same sphere. Then Eq. (12) can be written as

$$a_N \left[1 + f_{\text{MOND}}(a/a_c) \right] = a . \quad (15)$$

Solving this equation for the acceleration a will also determine $M' = M f_{\text{MOND}}(a/a_c)$. The dark matter distribution determined in this fashion would precisely reproduce the results of MOND without modifying inertia or the law of gravity.

Note, however, that this type of dark matter can be expected to be quite different from any other type of dark matter heretofore considered, be it cold, warm, hot, or mixed. First, M' is proportional to M , so the dark matter must track the baryonic matter. Second, M' is dependent on a_c . This can be interpreted as due to the dark matter being knowledgeable about the Hubble parameter $H_0 \approx 2\pi a_c/c$. Third, the dependence on a , which must be introduced to cancel the dimensions of a_c by taking the ratio a/a_c , but is a parameter that must be determined by solving the equation of motion, means that the dark matter distribution is closely linked to the consistency of the dynamics.

As far as the knowledge of $a_c \sim cH_0$ is concerned, [Kaplinghat & Turner \(2002\)](#) have argued that the acceleration scale cH_0 may arise naturally within CDM models if one considers the energy dissipation (cooling) and collapse of baryonic matter into the central regions within galactic CDM haloes (which do not collapse). Because of the baryonic collapse, gravity in the central regions of galaxies is dominated by baryonic gravity, while that in the outskirts is dominated by CDM gravity. Due to the scaling properties of this process, cH_0 is argued to set a universal scale at which this transition occurs. For clusters, on the other hand, gravity is everywhere CDM dominated and this transition does not occur, explaining the failure of MOND. In the [Kaplinghat & Turner \(2002\)](#) approach, therefore, the CDM obtains information on cH_0 from the simple fact that it is evolving in a universe expanding at the rate of H_0 , whereas

the coincidence $a_c \sim O(1)cH_0$ is more of a numerical accident. And even with this knowledge, CDM has problems at the galactic scale as mentioned above.

If a dark-matter model is to reproduce the success of MOND, two questions must be answered:

- (i) What should the function $f_{\text{MOND}}(x)$ appearing in Eq. (15) be?
- (ii) What dynamics must the dark-matter have to reproduce such a mass distribution?

Beginning with the first question, the asymptotics of the MOND interpolating function $\mu(x)$ only demand

$$f_{\text{MOND}}(x) = \begin{cases} 0 & (x \gg 1) \\ x^{-1} & (x \ll 1) \end{cases} \quad (16)$$

which is not much of a constraint. Also, though we are trying to reverse engineer MOND, one eventually wishes to predict MONDian behavior from a dark-matter model based on fundamental principles.

First and foremost, the dark matter must know about cH_0 via some fundamental principle and not by accident. To this end, [Ho, Minic & Ng \(2010, 2011, 2012\)](#) used standard gravitational thermodynamics, and Verlinde's idea of entropic gravity ([Verlinde 2011](#)), to argue that in a de Sitter space with cosmological constant Λ , the equation of motion should read

$$a_N \left[1 + f_{\text{MDM}}(a/a_0) \right] = \sqrt{a^2 + a_0^2} - a_0 , \quad (17)$$

where

$$\frac{M'}{M} = f_{\text{MDM}}(a/a_0) , \quad (18)$$

and a_0 is given by the cosmological constant Λ as

$$a_0 = c^2 \sqrt{\frac{\Lambda}{3}} = cH_0 = 2\pi a_c . \quad (19)$$

Despite its appearance, Eq. (17) does not modify General Relativity (GR) since the derivation of the right-hand-side is based on GR. The information on $cH_0 = c^2 \sqrt{\Lambda/3}$ is conveyed to the dark-matter via the temperature of the de Sitter horizon.

[Ho, Minic & Ng \(2010, 2011, 2012\)](#) dubbed the hypothetical dark matter which satisfies Eq. (17) 'MONDian Dark Matter' (MDM), but the equation of motion is distinct from Eq. (15).⁶ Unfortunately the name conjured among the community the idea that MDM was a hybrid theory, which it is not. We therefore choose to rename the model 'Modified Dark Matter' (MDM, same acronym) to clarify that it is a dark-matter model, albeit an exotic one.

As the MDM distribution function, [Ho, Minic & Ng \(2010, 2011, 2012\)](#) chose

$$f_{\text{MDM}}(a/a_0) = \frac{1}{\pi} \left(\frac{a_0}{a} \right)^2 , \quad (20)$$

which goes to zero in the limit $a \gg a_0$, and reproduces the flat galactic rotation curves. Note that $f_{\text{MDM}} \sim x^{-2}$ and not x^{-1} as in Eq. (16). As we will show in section 2, this form

⁶ This is the reason why it is inappropriate to translate the MDM distribution function into a MONDian interpolation function ([Edmonds et al. 2014](#)).

is suggested by the heuristic arguments based on gravitational thermodynamics presented in section 2. This choice is, of course, arbitrary and a case of reverse engineering. Ho, Minic & Ng (2012) proposed that quanta which obey infinite statistics (Doplicher, Haag & Roberts 1971, 1974; Govorkov 1983; Greenberg 1990; Shevchenko 2008) may exhibit the necessary dynamics to predict such behavior, but the details have yet to be worked out. We note in passing, however, that quanta of infinite statistics cannot be expressed as excitations of a local quantum field theory (QFT) and are intrinsically ‘non-local’ in nature, indicating that they have at least one feature that may be required of MDM.

Despite lacking a dynamical theory, which precludes performing numerical simulations, Edmonds et al. (2014) confronted the proposed MDM distribution with galactic rotation curves to see if it has merit from the phenomenological point of view. It was found that the MDM distribution does indeed provide a good fit to the data, and with a single fitting parameter (the mass to luminosity ratio of the galaxy) as opposed to three (two of which are correlated) for the well-known dark matter mass profile of Navarro, Frenk & White (1996) (NFW). This could indicate some hidden structure connected to the cosmological constant within the CDM mass profiles.

In this paper, we seek to extend our investigation of MDM to galaxy clusters. There, Eq. (20) is not expected to work, given that it closely resembles MOND which does not work either. We therefore begin by seeking a generalization of Eq. (20) which also places the expression onto a firmer theoretical footing. We then confront the galaxy cluster data to demonstrate the merit of the improved/generalized MDM distribution functions.

This paper is organized as follows. In section 2 we review our derivation of Eq. (17), based on gravitational thermodynamics, and provide a theoretical justification for the MDM profile proposed by Ho, Minic & Ng (2010, 2011, 2012) and studied by Edmonds et al. (2014), albeit with a slight rescaling. In section 3, we generalize the MDM mass profile to account for galaxy cluster data as well as galactic rotation curves and confront the new distribution with the virial mass profiles of 13 low-redshift, relaxed galaxy clusters. Section 4 is devoted to summary and discussion. In the appendix we present the successful fit of the generalized MDM mass profile to galactic rotation curves. We find that the MDM mass profile is sensitive to the cosmological constant on both the cluster and galactic scales. This in turn may constrain the nature of CDM.

2 THE MODIFIED DARK MATTER MASS PROFILE

2.1 Background

As mentioned above, the missing mass problem in the context of Einstein’s equation $G_{\alpha\beta} = (8\pi G)T_{\alpha\beta}$ can be solved in two ways: change the source $T_{\alpha\beta}$ by adding a new energy-momentum tensor, or change the Einstein tensor $G_{\alpha\beta}$. CDM is an example of the first option, one in which the extra energy momentum tensor is independent of the original baryonic tensor. The second option is a modification of gravity. Modifications to inertia, such as in Milgrom’s scaling, should

naturally emerge from this second option (e.g. Bekenstein 2004). However, one could also recast Einstein’s equation such that the energy-momentum part contains the cosmological constant term, $\Lambda g_{\alpha\beta}$, and the question arises whether the CDM mass profiles could know about the cosmological constant. This is the idea of modified dark matter (MDM).

Given the nature of the cosmological constant problem, the MDM approach should, at heart, be based on quantum gravity. However, quantum gravity is a very difficult problem; So our proposal is to look at the thermodynamic reformulation of Einstein’s theory and search for a commensurate modification of the energy momentum tensor that accounts for the cosmological constant. The reason for this is that gravitational thermodynamics (the prototype of which is black hole thermodynamics) is the only place where quantum theory and physics in accelerating frames are (currently) precisely related.

2.2 Gravitational Thermodynamics

In presenting this idea we follow the approach of Jacobson (1995). We consider a local observer with acceleration a in a spatially flat de Sitter space (i.e. one dominated by a positive cosmological constant Λ , in which $a_0 = c^2\sqrt{\Lambda/3}$ and $\Lambda = 3H_0^2/c^2$). In such a space, the thermodynamic relation

$$dE = TdS \quad (21)$$

has T as the Unruh temperature associated with the local accelerating (Rindler) observer (Davies 1975; Unruh 1976)

$$T = \frac{\hbar a}{2\pi c k_B}. \quad (22)$$

The acceleration a can be interpreted as surface gravity on the associated (Rindler) horizon. The entropy S is then associated with the area of this horizon⁷

$$S = \frac{c^3 A}{4G\hbar}, \quad (23)$$

and the energy E is the integral of the energy momentum tensor

$$E = \int T_{\alpha\beta} k^\alpha k^\beta \quad (24)$$

where k^α are appropriate unit vectors.

The link between this thermodynamic equation and Einstein’s equations is given by the Raychaudhuri equation.⁸ For an instantaneously stationary local Rindler horizon the shear and vorticity terms can be neglected, effectively leaving:

$$\frac{\delta A}{\delta \lambda} = R_{\alpha\beta} k^\alpha k^\beta + \dots \quad (25)$$

where λ is the appropriate affine parameter and k^α are the unit tangent vectors to the appropriate geodesic whose cross sectional area A is being focused.

⁷ This scaling of entropy with area is sometimes called “holography” (’t Hooft 1993; Susskind 1995).

⁸ Used by Penrose and others to discuss gravitational focusing in their seminal proofs of the singularity theorems (Penrose 1965).

Taking the above expressions, along with the expressions for the Hawking-Unruh temperature T and the Bekenstein-Hawking entropy S , it then follows that

$$8\pi G \int T_{\alpha\beta} k^\alpha k^\beta = \int R_{\alpha\beta} k^\alpha k^\beta \quad (26)$$

and thus that $T_{\alpha\beta} \propto R_{\alpha\beta} - f g_{\alpha\beta}$. The local divergenceless of $T_{\alpha\beta}$ then sets $f = -R/2 + \Lambda$ (via the Bianchi identity), and we recover Einstein's equations. Even the correct factor of $8\pi G$ comes from the factor of 2π , the periodicity of the euclidean time in the temperature formula, and the $4G$ from the entropy formula. The local acceleration, a , in this context just sets the correct units between the entropy and energy.

Our modification to Jacobson's argument is to *introduce a fundamental acceleration that is related to the cosmological constant*. Since we wish to preserve the holographic scaling of the area (to remain consistent with Einstein's theory) and still have a standard energy-momentum tensor, we are compelled to change something in the thermodynamic expression that can be interpreted both from the point of view of inertia and from the point of view of a mass source. We must therefore preserve the entropy but change the temperature such that the additional part of the energy momentum tensor "knows" about the inertial properties that temperature knows about. This corresponds to a change in Equation (21) such that the change in temperature amounts to a particular change in energy that leaves the entropy unchanged. The constancy of the entropy dS is a form of infinitesimal adiabaticity.

To change the temperature we turn to our local observer with acceleration a in de Sitter space, and thus with total acceleration $a_0 + a$ (where $a_0 = c^2 \sqrt{\Lambda/3}$). The Unruh temperature experienced by this observer is (Deser & Levin 1997; Jacobson 1998)

$$T_{a_0+a} = \frac{\hbar}{2\pi c k_B} \sqrt{a^2 + a_0^2}. \quad (27)$$

However, since de Sitter space has a cosmological horizon, it has a horizon temperature associated with a_0 . We thus define the following *effective* temperature, so that for zero acceleration we get zero temperature

$$\tilde{T} \equiv T_{a_0+a} - T_{a_0} = \frac{\hbar}{2\pi c k_B} \left(\sqrt{a^2 + a_0^2} - a_0 \right). \quad (28)$$

This reduces to the usual temperature for Rindler observers by neglecting a_0 . Note that

$$\sqrt{a^2 + a_0^2} - a_0 \approx \begin{cases} a & (a \gg a_0), \\ \frac{a^2}{2a_0} & (a \ll a_0). \end{cases} \quad (29)$$

Our model is thus:

$$d\tilde{E} = \tilde{T} dS, \quad (30)$$

in which dS remains unchanged and where we define, in analogy with the normalized temperature \tilde{T} , the normalized energy

$$\tilde{E} = E_{a_0+a} - E_{a_0}. \quad (31)$$

Therefore, energy is not changed in an arbitrary way, but instead in accordance with the change in temperature that should be fixed by the background.

If we now require that $a = a_N$, so that we have *locally* what Einstein's theory would give in the Newtonian limit, then we have, at least from the point of view of the temperature, Milgrom's scaling. There is, however, a key advance in our argument: Milgrom's scaling emerges as the difference between the temperature of an accelerated observer in de Sitter space and the background temperature of the cosmological horizon, in the limit of accelerations small compared to the acceleration associated with the surface gravity of the cosmological horizon. Milgrom's scaling (MOND) ($a = a_N$, $a \gg a_c$ and $a = \sqrt{a_N a_c}$, $a \ll a_c$) sets the value of a_c from the Hubble scale; a_0 is related to Milgrom's critical acceleration a_c as $a_c = a_0/(2\pi)$ (Milgrom 1983a,b,c).

2.3 The MDM Mass Profile

How does this argument relate to the idea of 'missing' mass? It follows from Equation (30) that

$$dE_{a_0+a} = T_{a_0+a} dS, \quad (32)$$

where the entropy S is still given by Equation (23), so that the Einstein tensor is untouched. However, due to the change in temperature the energy is changed. If we rewrite the temperature as $T_{a_0+a} = T + T'$ where the T part corresponds to the Unruh temperature of the observer moving with the Newtonian acceleration a_N (in the correspondence limit $a_0 \ll a = a_N$), then we can also write

$$dE + dE' = T dS + T' dS. \quad (33)$$

If we interpret the original $dE = T dS$ as corresponding to baryonic matter, then

$$dE' = T' dS = \frac{T'}{T} dE. \quad (34)$$

Thus the energy momentum tensor of the extra sources (which we will identify with missing mass) has to be related to the energy momentum tensor of ordinary visible matter (via equation (24)).

Finally, by expanding the formula for the de Sitter temperature we have a relation between the energy momentum tensors of the dark (prime) and visible (unprime) matter

$$T'_{\alpha\beta} = \frac{a_0^2}{2a^2} T_{\alpha\beta}, \quad (35)$$

which for energy density (i.e. the 00 components) is

$$M' = \frac{a_0^2}{2a^2} M. \quad (36)$$

The M' in the above expression is what we call 'dark matter.' This dark matter profile is similar to the one in our original papers on MDM (Ho, Minic & Ng 2010, 2011, 2012), but with the appearance of the factor of 1/2 as opposed to the original $1/\pi$ (which was motivated by the Tully-Fisher relation). The exact forms, without any expansion, are

$$T'_{\alpha\beta} = \left(\sqrt{1 + \frac{a_0^2}{a^2}} - 1 \right) T_{\alpha\beta}, \quad (37)$$

and

$$M' = \left(\sqrt{1 + \frac{a_0^2}{a^2}} - 1 \right) M, \quad (38)$$

respectively. This gives rise to the idea of ‘entropic force’, where:

$$F_{\text{entropic}} = m \left(\sqrt{a^2 + a_0^2} - a_0 \right), \quad (39)$$

and

$$\sqrt{a^2 + a_0^2} - a_0 = \frac{G(M + M')}{r^2}, \quad (40)$$

respectively.

Our dark matter mass profile thus “knows” about the visible matter as well as the cosmological background, and it also knows about the inertial properties of the moving masses in that background, since it is directly tied to the visible matter, the cosmological constant $\Lambda \equiv 3a_0^2/c^2$, and the inertial properties (acceleration a). In essence, we have a vacuum origin of the fundamental acceleration and also a quantum origin of the mass profile that could lead to the observed galactic rotation curves. From our perspective, flat galactic rotation curves are a quantum gravity effect at large scales.

3 GALAXY CLUSTERS

3.1 MDM Distribution Function for Clusters

In principle, the above mass profile, Eq. (36), fixed by the ratio of the corresponding Unruh-Hawking temperatures (in the limit of small a_0/a) can be modified due to some well-known physical effects associated with a change of scale. For example, the temperature can be changed via the Tolman-Ehrenfest formula (Tolman 1930; Tolman & Ehrenfest 1930)

$$T\sqrt{g_{00}} = 2\tilde{\alpha}, \quad (41)$$

where the g_{00} is essentially determined by the gravitational potential Φ , $g_{00} = 1 + 2\Phi$ (in the units $c = 1$), and the dimensionful factor $\tilde{\alpha}$ is determined by the boundary conditions of the problem.

The questions are what gravitational potential should be used in our case and what sets the value of $\tilde{\alpha}$. For example, for a constant background gravitational field, i.e. the linear potential, we are led to consider the following modification of the mass profile:

$$f_{\text{MDM}}(a/a_0) = \frac{M'}{M} = \frac{\alpha}{[1 + (r/r_{\text{MDM}})]} \left(\frac{a_0}{a} \right)^2, \quad (42)$$

where the dimensionless factor α is really determined by the ratio of dimensionful $\tilde{\alpha}$ at different scales (in our case, the cluster and galactic scales). It is interesting that the same prefactor can be obtained in the context of conformal gravity by rewriting the FRW cosmological line element in the Schwarzschild coordinate system (the linear potential also being the direct analogue of the Newtonian potential for conformal gravity; see Mannheim & O’Brien 2013). Note that the prefactor $\alpha/[1 + (r/r_{\text{MDM}})]$ is only the leading term in a more general expression that involves higher order terms in r .

Regarding the value of α we note that the boundary value of the temperature is set by the ratio $a_0^2/2a^2$, which scales as distance squared, because $a \sim 1/r$. Thus, in principle, α can increase with distance. However, our argument is too heuristic to determine the form of this scaling.

In what follows we show that the mass profile given in Equation 42 very nicely fits the cluster data and reproduces the relevant virial mass profile, with $\alpha \sim 100$ and $r_{\text{MDM}} \sim 10$ Kpc. However, on galactic scales, given our previous successful fits of the galactic rotation curves, $\alpha \sim 1$ and also r is much smaller than r_{MDM} . Thus, in going from the galactic to the cluster scales, α needs to change by two orders of magnitude. This is not completely unrealistic, given our heuristic thermodynamic reasoning, but we have to admit of being ignorant of the underlying reason for this.

3.2 Comparison to Galaxy Cluster Data

We compare MDM mass profiles with the observed (virial) mass profiles in a sample of 13 relaxed galaxy clusters given in Vikhlinin et al. (2006). This sample was chosen for several reasons. Firstly, they analyzed all available *Chandra* data which were of sufficient quality to determine mass profiles robustly out to large radii ($\sim 0.75r_{500}$ and extended past r_{500} in five clusters), spanning a temperature range of 0.7 – 9 keV. This provides us with a significant sample size with data covering radii from the inner, cooling region out to the virial radius. Secondly, their fitting models were given enough degrees of freedom to get very accurate data fits, which allows us to compare MDM mass profiles to these very accurate models. Thirdly, whenever possible, data from two different X-ray observatories, *Chandra* and ROSAT, were compared and combined in order to ensure that derived cluster brightness profiles agree in the overlapping regions. At large radii, the *Chandra* field of view limits the statistical accuracy of surface brightness profiles. To overcome this problem, Vikhlinin et al. (2006) combined ROSAT-PSPC and *Chandra* data in cases where the PSPC observations were sufficiently deep (see Table 1, adapted from Vikhlinin et al. 2006). The main goals of the analysis were to extract accurate temperature profiles and surface brightness profiles out to a large fraction of the virial radius. Spectral analysis to obtain temperature profiles is presented in Vikhlinin et al. (2005), and details of the X-ray surface brightness profiles is presented in Vikhlinin et al. (2006).

The observed mass profiles are inferred from temperature (T) and gas density (ρ_g) measurements assuming spherical symmetry and hydrostatic equilibrium (Sarazin 1988):

$$M(r) = -\frac{k_B T(r)r}{\mu m_p G} \left(\frac{d \ln \rho_g(r)}{d \ln r} + \frac{d \ln T(r)}{d \ln r} \right), \quad (43)$$

where k_B is Boltzmann’s constant, m_p is the mass of a proton, and $\mu \approx 0.6$ is the mean molecular weight for a plasma with primordial abundances.

The vast majority of the baryons in galaxy clusters are contained in a hot, diffuse gas ($T > 10^6$ K and densities ~ 0.3 particles per cubic centimeter). In such conditions, the primary emission process is due to thermal *bremssstrahlung*. Recombination of electrons with heavier elements also contributes to the X-ray spectrum allowing for measurements of the ionization and chemical abundances of the plasma. The traditional model for the gas density in galaxy clusters is given by (Cavaliere & Fusco-Femiano 1978)

$$n_e n_p = \frac{n_0^2}{[1 + (r/r_c)^2]^{3\beta}}. \quad (44)$$

To better fit the observed surface brightnesses of galaxy clusters in our sample, the gas density is modified to be

$$n_e n_p = \frac{n_0^2 (r/r_c)^{-\alpha}}{[1 + (r/r_c)^2]^{3\beta - \alpha/2} [1 + (r/r_s)^\gamma]^{\varepsilon/\gamma}} + \frac{n_{02}^2}{[1 + (r/r_{c2})^2]^{3\beta_2}}. \quad (45)$$

These modifications to the traditional model provide a cusp in the center of the galaxy cluster ($r < r_c$), a steeper X-ray brightness profile at large radii ($r > r_s > r_c$), and extra modeling freedom near the centers of clusters ($r < r_{c2} < r_c$) (Vikhlinin et al. 2006). The gas mass density is then given by

$$\rho_g = 1.24 m_p \sqrt{n_e n_p}, \quad (46)$$

for the plasma with primordial helium abundance and a metallicity of $0.2Z_\odot$ for heavier elements.

Temperature profiles in the inner regions of galaxy clusters differ from those in the outer regions, and these regions must be modeled separately. Toward the cluster center, temperatures decline. Temperatures in the cooling region are described by (Allen et al. 2001; Sanders and Fabian 2002; Burns, Skillman & O’Shea 2010; Moretti et al. 2011)

$$t_{\text{cool}}(r) = \frac{(r/r_{\text{cool}})^{a_{\text{cool}}} + T_{\text{min}}/T_0}{1 + (r/r_{\text{cool}})^{a_{\text{cool}}}}. \quad (47)$$

Outside of the cooling region, the temperature profile can be modeled as a broken power law,

$$t(r) = \frac{(r/r_t)^{-a}}{[1 + (r/r_t)^b]^{c/b}}. \quad (48)$$

The three-dimensional temperature profile is described by the product of these two models (Vikhlinin et al. 2006),

$$T_{3D}(r) = T_0 t_{\text{cool}}(r) t(r). \quad (49)$$

3.3 Data fits of mass profiles

The dark matter mass profile predicted by MDM is given by Equation (42). The total mass, the sum of dark matter and baryonic matter, is compared with the virial mass for each galaxy cluster. The data fits are depicted in Figure 1 with results provided in Table 1. Based on the analysis of Vikhlinin et al. (2006), we have assigned a $1\text{-}\sigma$ error of 10% on the virial mass determinations indicated by the shaded regions in the figure. While function parameter errors were not reported, inspection of their figures 3 – 15 indicate that 10% is a reasonable estimate. They also mention in the text that Monte Carlo simulations suggest statistical errors in gas density determinations of $\lesssim 9\%$.

For comparison, we include dynamical masses predicted by CDM and MOND. For CDM, we use the Navarro, Frenk & White (1996) (NFW) density profile,

$$\rho_{\text{NFW}}(r) = \frac{\rho_0}{\frac{r}{r_{\text{CDM}}} \left(1 + \frac{r}{r_{\text{CDM}}}\right)^2}, \quad (50)$$

to determine the mass predicted by CDM, where

$$r_{\text{CDM}} = \frac{r_{200}}{c}, \quad (51)$$

and r_{200} designates the edge of the halo, within which objects are assumed to be virialized, usually taken to be the

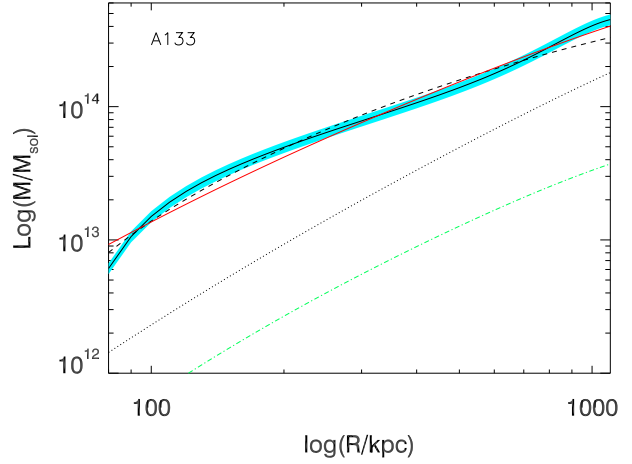


Figure 1. Plots of total mass within radius R (assuming spherical symmetry). The solid black line is the virial mass; The shaded region surrounding the virial mass plot represents the $1\text{-}\sigma$ error, estimated at 10% from the analysis of Vikhlinin et al. (2006); The dot-dashed green line is gas mass; The dotted black line is MOND (effective mass); The dashed black line is CDM; The solid red line is MDM with $\alpha = 100$.

boundary at which the halo density exceeds 200 times that of the background. The parameter c (not to be confused with the speed of light) is a dimensionless number that indicates how centrally concentrated the halo is.

For MOND, we have from Eq. (14)

$$\frac{M'(r)}{M(r)} = f_{\text{MOND}}(a(r)/a_c) = \frac{1}{\mu(a(r)/a_c)} - 1, \quad (52)$$

where $M(r)$ and $M'(r)$ are respectively the total baryonic and dark matter mass enclosed within a sphere of radius r around the center of the cluster. Assuming a spherically symmetric distribution, the dark matter density profile is then

$$\rho_{\text{MOND}}(r) = \frac{1}{4\pi r^2} \frac{d}{dr} M'(r). \quad (53)$$

This dark matter profile $\rho_{\text{MOND}}(r)$ will reproduce the acceleration profile $a(r)$ for a given MOND interpolating function $\mu(x)$. We use the interpolating function given in Eq. (4) with $n = 1$ (Famaey & McGaugh 2012), instead of the $n = 2$ case originally proposed by Milgrom (1983a,b,c) and used by Sanders (1999, 2003) to fit cluster data, since it seems to provide better fits.

We see in Figure 1 that the MDM mass profiles fit the virial mass data well. The fits for MDM mass profiles are as good as those for NFW. The MOND (effective) mass profiles fail to reproduce the virial mass profiles both in magnitude and in shape; The mass discrepancy in the MOND model is more significant in the inner regions of the cluster than in the outer regions.

4 DISCUSSION

In this paper we have presented further observational tests of Modified Dark Matter (MDM) by fitting the MDM mass profile to 13 low-redshift, relaxed X-ray-emitting clusters of

Table 1. Sample of galaxy clusters with redshifts as given in Vikhlinin et al. (2006). For each cluster, the baryonic, MDM (using $\alpha = 100$) and CDM masses contained within the observed radii are given in columns 3 – 5, respectively. The scale radius r_{MDM} for MDM is given in column 6 and columns 7 and 8 contain the fitting parameters (concentration and scale radius) for the NFW mass profile. We note that MOND has no mass term other than the baryonic mass and uses no free fitting parameters.

Name	z	M_{B} ($10^{12} M_{\odot}$)	M_{MDM} ($10^{12} M_{\odot}$)	M_{CDM} ($10^{12} M_{\odot}$)	r_{MDM} (kpc)	c	r_{CDM} (kpc)
A133	0.0569	5.5	12.9	17.1	0.818	3.75	200
A262	0.0162	3.2	38.6	34.9	10.3	6.00	167
A383	0.1883	11	87.5	93.5	17.9	6.81	241
A478	0.0881	18	106	110	16.3	6.82	263
A907	0.1603	11	106	103	25.5	7.48	225
A1413	0.1429	13	126	116	31.7	7.85	226
A1795	0.0622	12	85.4	98.9	15.5	6.14	284
A1991	0.0592	4.3	54.4	54.1	15.6	6.86	178
A2029	0.0779	16	147	143	39.7	8.39	231
A2390	0.2302	19	116	111	18.5	8.02	214
RX J1159+5531	0.0810	41.3	17.6	38.0	19.0	6.18	169
MKW 4	0.0199	2.0	36.3	33.9	14.4	6.04	164
USGC S152	0.0153	0.95	14.3	13.5	4.42	5.36	119

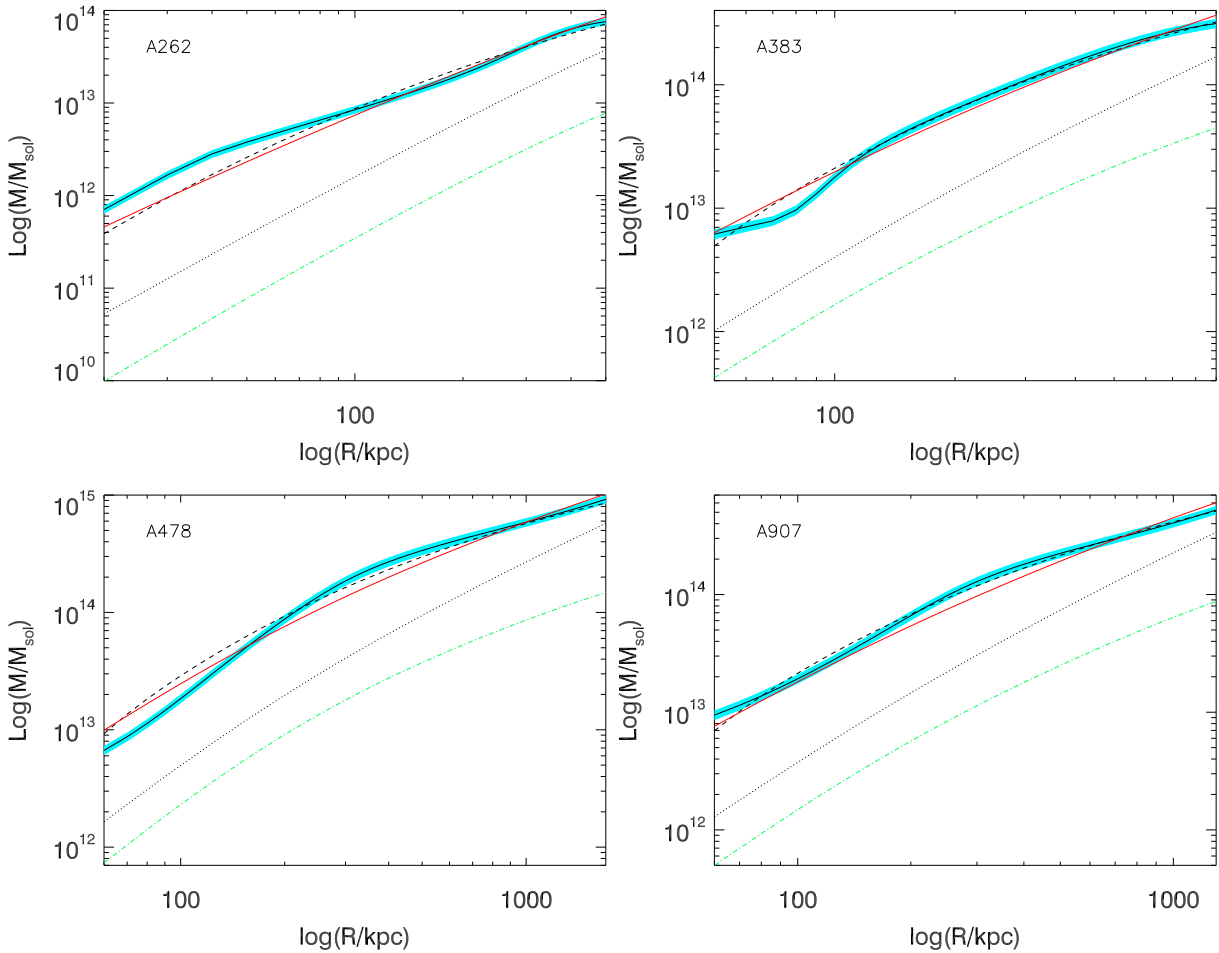
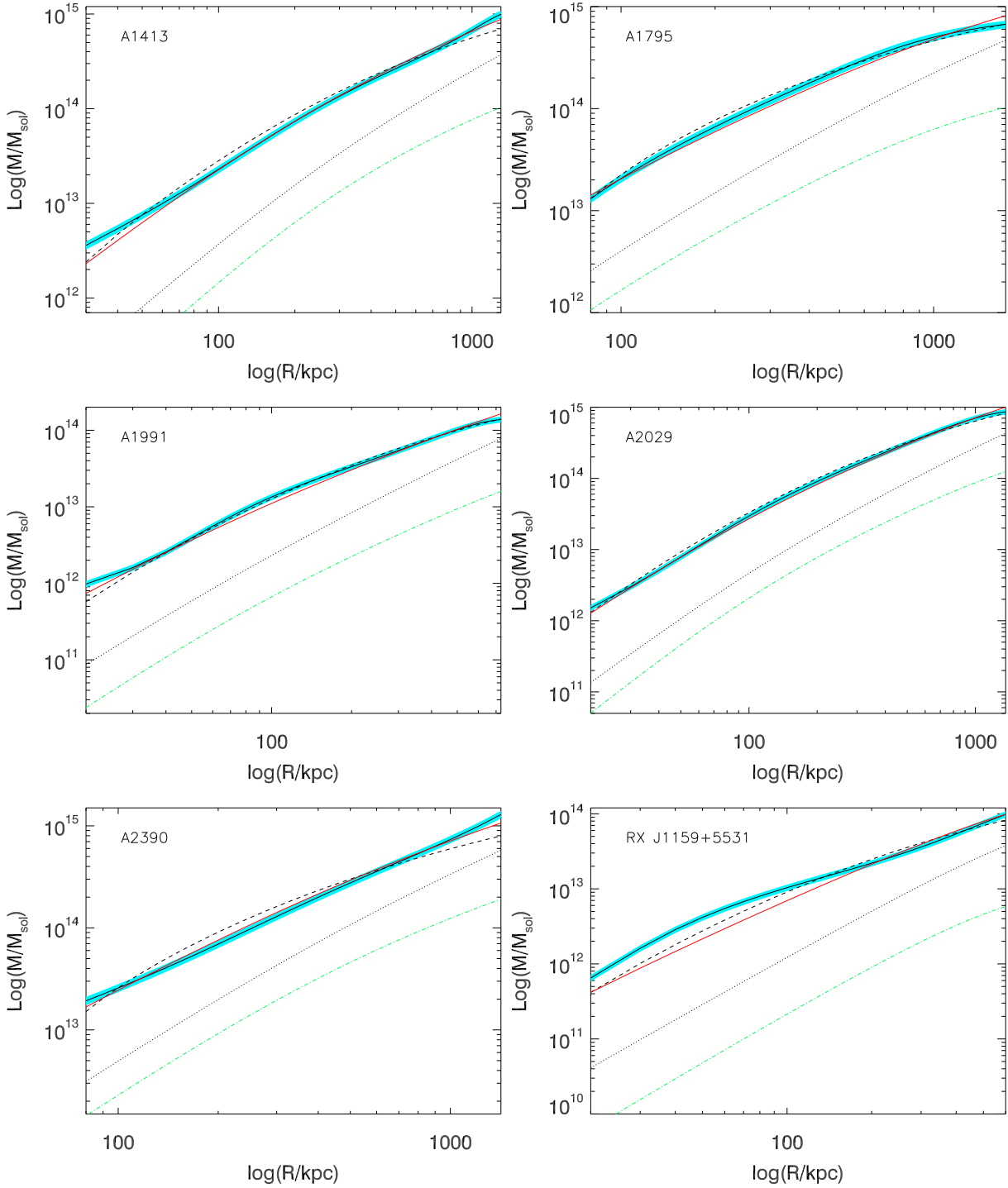


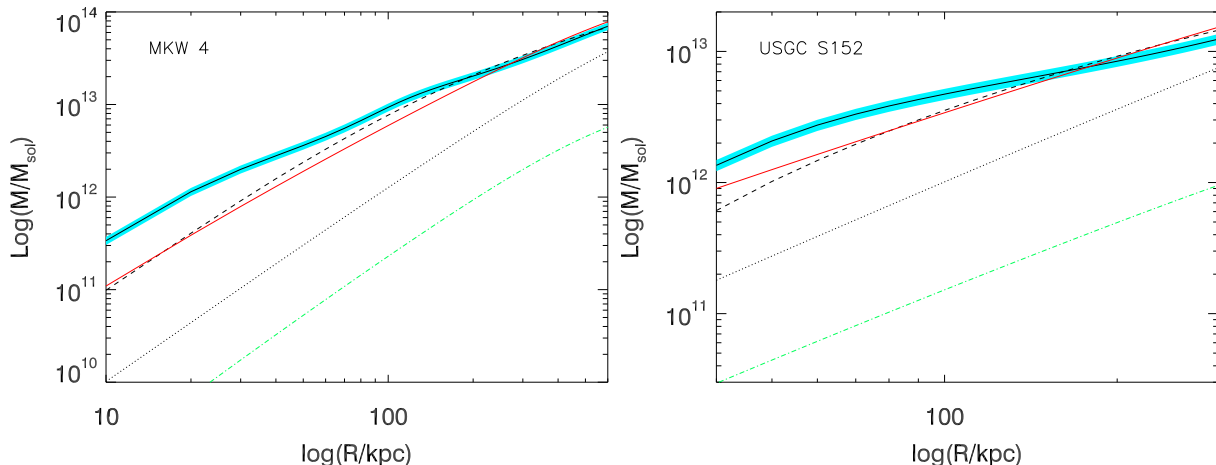
Figure 1 – continued

Figure 1 – *continued*

galaxies. We have shown that MDM performs as well as CDM, and considerably better than MOND (which only works well at the galactic scale), for all clusters in our sample. Moreover, using arguments from gravitational thermodynamics, we have justified, on theoretical grounds, our MDM mass profile. Perhaps the most interesting aspect of our work is the dependence of the CDM mass profile on the cosmological constant. We suggest that the CDM mass pro-

files can be reorganized in a form suggested by the MDM mass profile. Such reorganization may constrain the nature of cold dark matter.

In Edmonds et al. (2014), we fit the MDM mass profile in Equation (20) to galactic rotation curves which differs from the one used for galaxy clusters in this paper by a function of radius (see Equation 42). In the appendix, we show that the generalized mass profile in Equation (42) also

Figure 1 – *continued*

works well for galactic rotation curves, albeit with a different constant scale value; $\alpha \sim 100$ for galaxy clusters and $\alpha \sim 1$ for galactic rotation curves. We do not yet know the underlying reason for the change in α , though, as discussed in section 3, α may be related to boundary conditions and can, in principle, scale with radius. Perhaps studying objects of similar scale, but under different physical conditions will be illuminating. The galaxy clusters in our sample were all low-redshift, virialized clusters. It would be interesting to constrain MDM mass profiles in clusters at higher redshifts, before they become virialized, assuming we can get reliable mass estimates in the non-virialized regions.

Along with the current work, we plan to study the constraints from gravitational lensing and colliding clusters such as the Bullet Cluster (1E 0657-558) and the Train Wreck Cluster (A520) on MDM. We will also test MDM at cosmic scales by studying the acoustic peaks in the CMB. In all of these follow-up studies, we will try to identify some distinctive observational signatures between MDM and CDM models.

Last but not least, it will be interesting and important to have a deeper understanding of the fundamental nature of the MDM quanta. We would like to construct explicit models of MDM quanta along the lines indicated by the logic of gravitational thermodynamics. The deeper nature of such quanta should be found in the context of quantum gravity. For example, such unusual non-local quanta could be found in recent reformulations of quantum gravity and string theory (Freidel, Leigh & Minic 2013, 2014, 2015). A more concrete theory for MDM quanta will allow us to test this idea at colliders, dark matter direct detection experiments and indirect detection experiments. For instance, we have speculated that the MDM quanta obey infinite statistics rather than the familiar Bose or Fermi statistics (Ho, Minic & Ng 2012; Greenberg 1990; Shevchenko 2008); This may lead to unusual particle phenomenology.

ACKNOWLEDGMENTS

We are grateful for helpful discussions with J. Beacom, C. Frenk, S. Horiuchi, J. Khoury, P. Mannheim and J. Mof-

fat. We are also grateful to the organizers of the Miami winter conference for providing an inspiring environment for work. CMH was supported in part by the Office of the Vice-President for Research and Graduate Studies at Michigan State University. YJN was supported in part by the Bahnsen Fund of UNC. DM was supported by the U.S. Department of Energy under contract DE-FG02-13ER41917, Task A.

APPENDIX A: GALACTIC ROTATION CURVES

In Edmonds et al. (2014), we fit a sample of galactic rotation curves using the MDM mass profile Equation (20). While this profile works well for galaxies, it does not fit the galaxy cluster data well. In this paper, we introduced a mass profile that works well for galaxy clusters (Equation 42), and we would like to see if the new mass profile can work at galactic scales as well as it does at cluster scales.

For the galaxy clusters in our sample, we found $\alpha \sim 100$ is required for the mass profile given in Equation (42). Since the fits to galactic rotation curves presented in Edmonds et al. (2014) were fit so well with Equation (20), we expect $\alpha \sim 1$ with $r_{\text{MDM}} \gg r$ in the generalized mass profile. The mass-to-light ratio (M/L) is unknown, and is therefore determined by data fits. The solution space is not well-constrained if we allow α and r_{MDM} to be fitting parameters in addition to M . Therefore, we fix the scale radius to be similar to those found for NFW halos; $r_{\text{MDM}} = 20$ kpc. It is interesting to note that this radius is near the observed turnover radius for the Milky Way (Merrifield 1992; Battaner & Florido 2000). However, the very extended rotation curve (~ 100 kpc) observed in UGC 2885 first drops, but then rises again to remain flat beyond 50 kpc. If more data at very large radii becomes available, it may be possible to constrain the scale radius in dark matter profiles.

With the scale radius and the constant scale factor α fixed to 20 kpc and 0.5, respectively, we reproduce the plots from Edmonds et al. (2014) using Equation 42 in Figure A1. In Table A1, we provide M/L , the mass of the dark matter component, and the baryonic mass (inferred from M/L).

Table A1. Sample of galaxies from Sanders (1996). Asterisks denote galaxies with disturbed velocity fields (Sanders 1996). Low-Surface-Brightness galaxies (LSBs) are marked with an (L), and the rest are High-Surface-Brightness galaxies (HSBs). For each galaxy, the baryonic and MDM masses contained within the observed radii are given in columns 2 and 3, respectively. The mass-to-light ratios (M/L) determined by fitting the MDM mass profile is given in column 4. This table is similar to Table 1 in Edmonds et al. (2014), but with values corresponding to the generalized MDM mass profile developed in this paper using $r_{\text{MDM}} = 20$ kpc and $\alpha = 0.5$.

Name	M_{B} ($10^{10} M_{\odot}$)	M_{MDM} ($10^{10} M_{\odot}$)	M/L (MDM) (M_{\odot}/L_{\odot})
NGC 3726	2.94	15.8	0.55
NGC 3769*	1.23	12.9	0.44
NGC 3877	3.17	3.67	0.53
NGC 3893*	3.95	9.19	0.73
NGC 3917 (L)	1.50	4.04	0.73
NGC 3949	1.46	1.43	0.45
NGC 3953	8.55	8.17	0.74
NGC 3972	0.944	1.63	0.63
NGC 3992	15.0	33.5	1.9
NGC 4010 (L)	0.909	2.06	0.48
NGC 4013	4.44	17.6	0.76
NGC 4051*	2.65	3.82	0.56
NGC 4085	0.832	0.982	0.50
NGC 4088*	3.72	9.73	0.43
NGC 4100	4.14	11.0	0.95
NGC 4138	2.55	6.83	0.80
NGC 4157	5.04	17.3	0.67
NGC 4183 (L)	0.946	5.28	0.59
NGC 4217	3.99	6.97	0.60
NGC 4389*	0.586	1.69	0.37
UGC 6399 (L)	0.257	0.832	0.60
UGC 6446 (L)	0.513	2.65	0.53
UGC 6667 (L)	0.235	0.801	0.53
UGC 6818* (L)	0.0997	0.484	0.30
UGC 6917 (L)	0.720	1.87	0.83
UGC 6923 (L)	0.172	0.415	0.42
UGC 6930 (L)	0.771	3.52	0.70
UGC 6973*	1.61	1.72	0.48
UGC 6983 (L)	0.869	3.45	1.1
UGC 7089 (L)	0.182	0.910	0.30

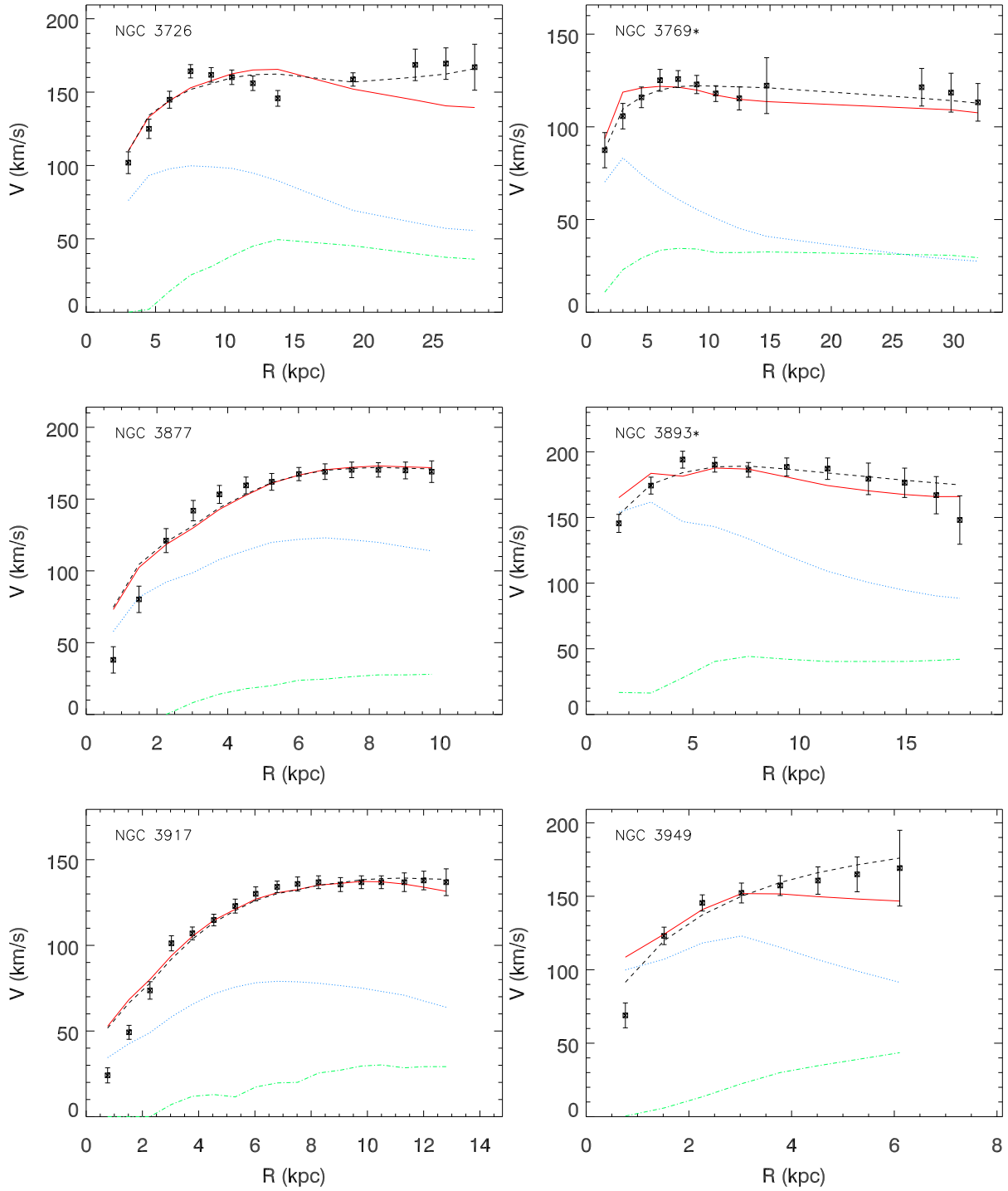


Figure A1. Galactic rotation curves. The observed rotation curve is depicted by points with error bars. The solid red and dashed black lines are the MDM and CDM rotation curves, respectively. Newtonian curves for the stellar and gas components of the baryonic matter are depicted by dotted blue and dot-dashed green lines, respectively. The mass of the stellar component is derived from the M/L ratio determined from MDM fits to the rotation curve. These figures are similar to those presented in [Edmonds et al. \(2014\)](#), but using the generalized mass profile presented in this paper using $r_{\text{MDM}} = 20$ kpc and $\alpha = 0.5$.

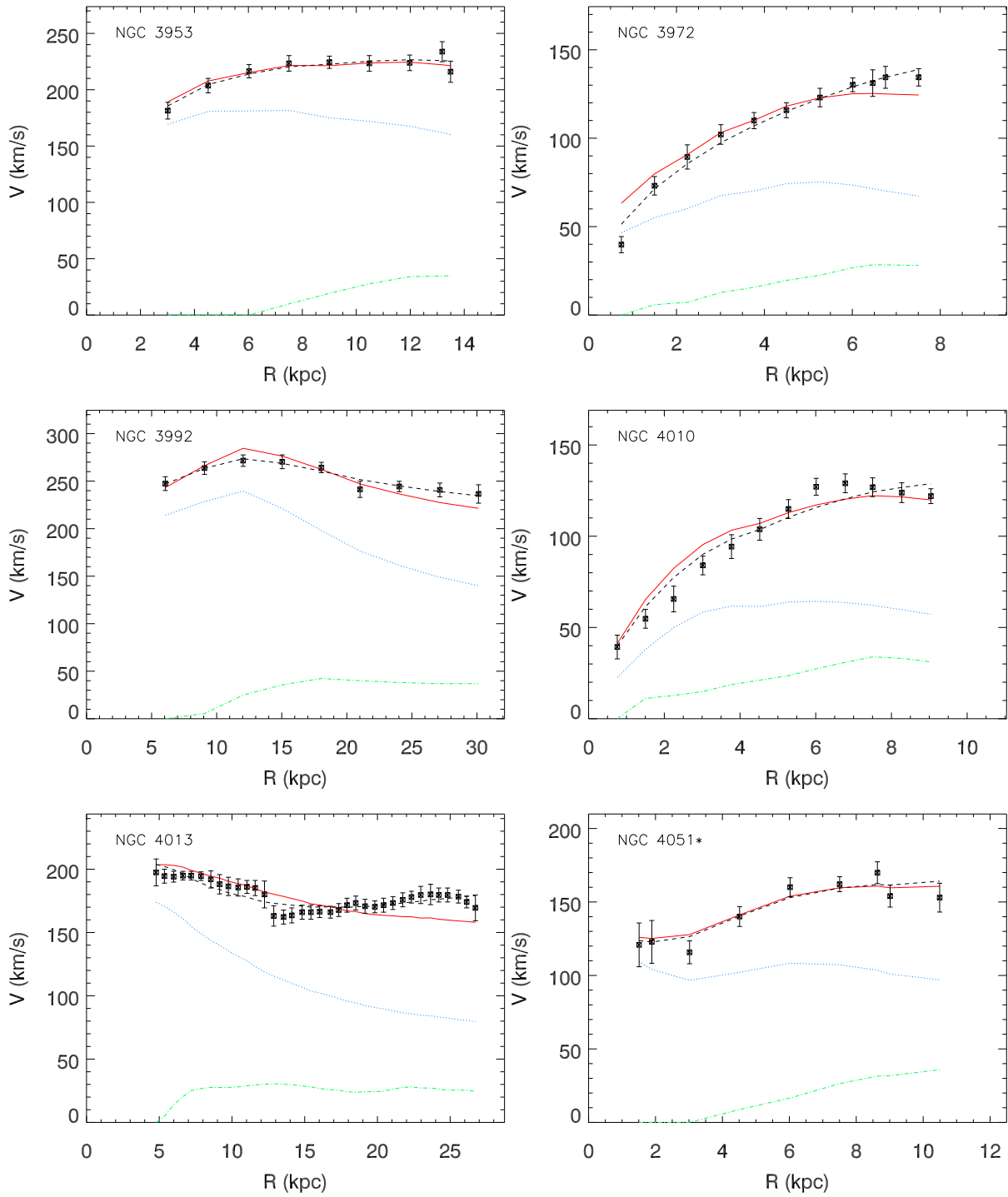


Figure A1 – continued

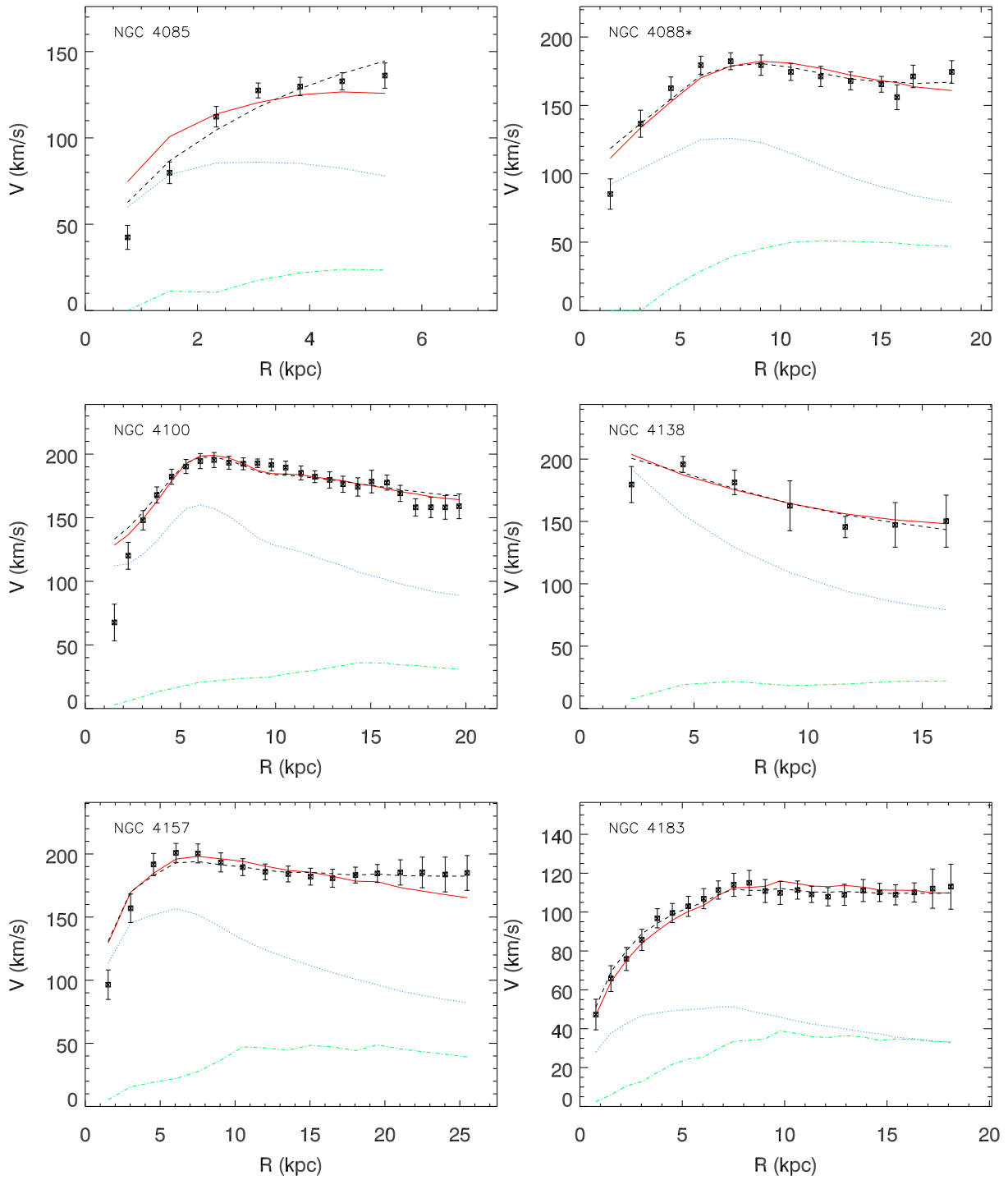


Figure A1 – *continued*

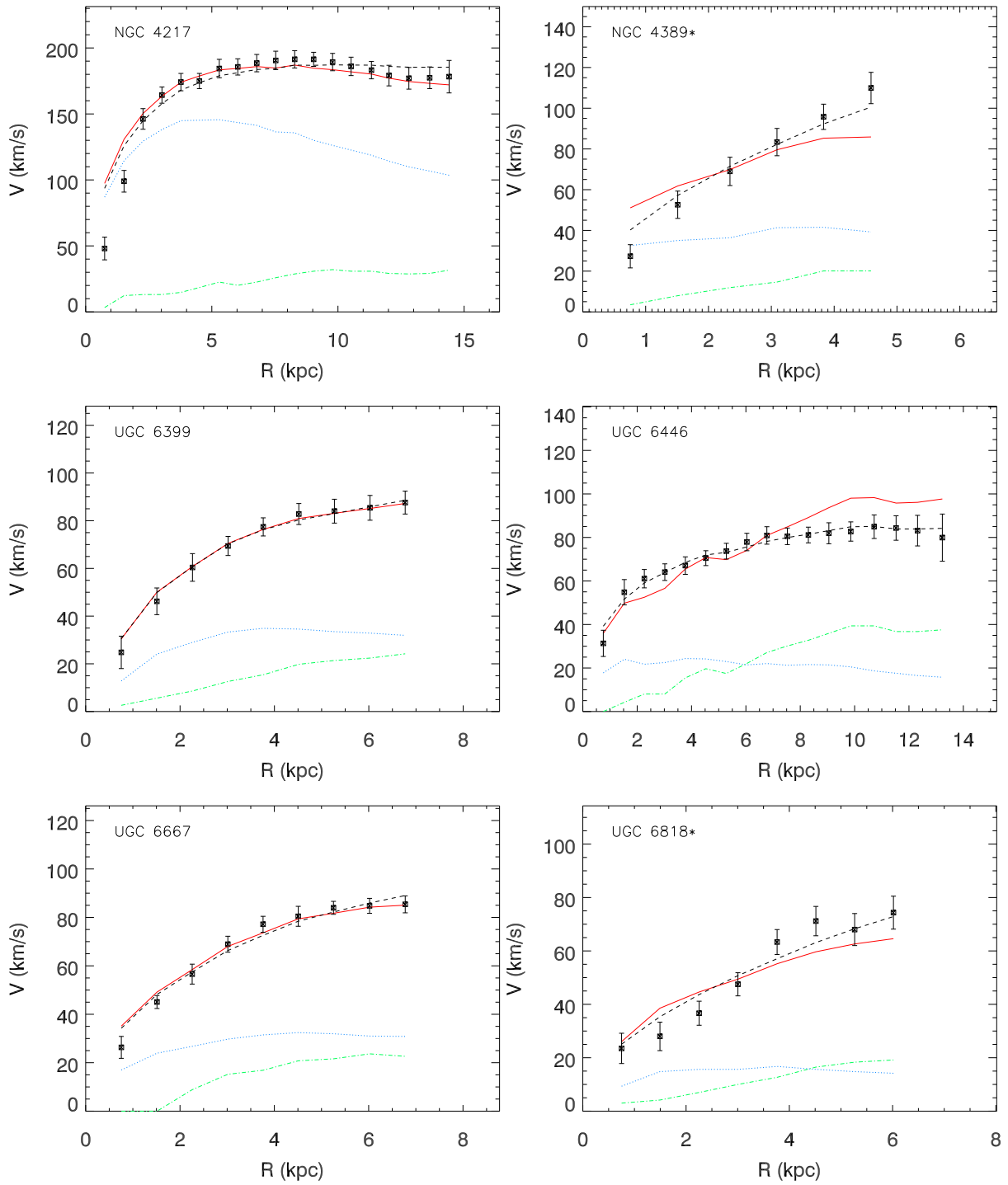


Figure A1 – continued

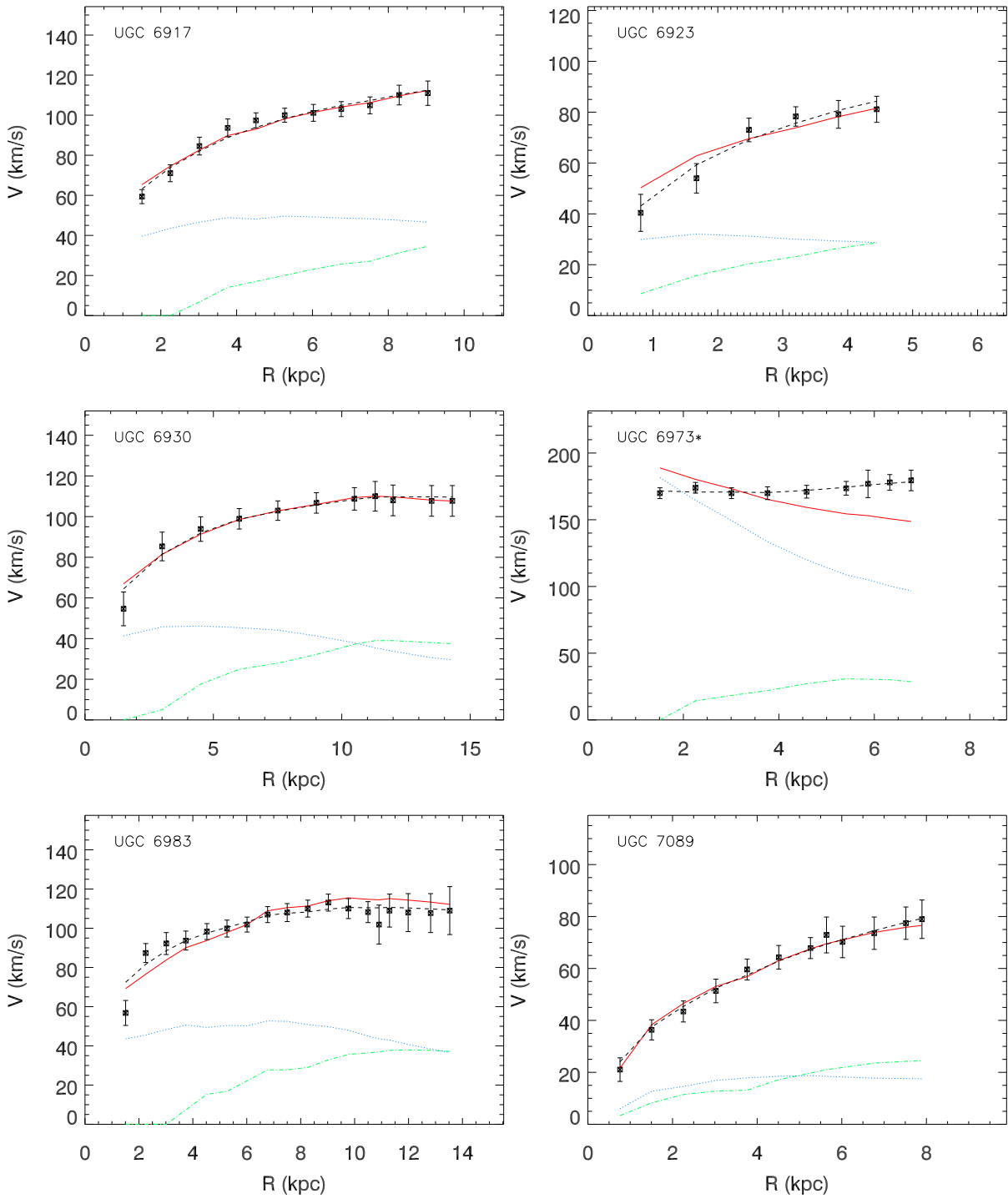


Figure A1 – *continued*

REFERENCES

- Ade P. A. R. et al. (Planck Collaboration), 2015, arXiv:1502.01589 [astro-ph.CO].
- Allen S. W., Fabian A. C., Johnstone R. M., Arnaud K. A. and Nulsen P. E. J., 2001, MNRAS, 322, 589.
- Battaner, E., & Florido, E. 2000, Fundamentals Cosmic Phys., 21, 1
- Begeman K. G., Broeils A. H. and Sanders, R. H., 1991, MNRAS 249, 523.
- Bekenstein J. D., 1973, Phys. Rev. D 7, 2333.
- Bekenstein J. D., 2004, Phys. Rev. D 70, 083509 [Erratum: 2005, Phys. Rev. D 71, 069901(E)].
- Berezhiani, L., & Khoury, J. 2015, Phys. Rev. D 92, 103510
- Bertone G., Hooper D. and Silk J., 2005, Phys. Rept. 405, 279 and references therein.
- Blanchet L. and Le Tiec A., 2008, Phys. Rev. D 78, 024031.
- Blanchet L. and Le Tiec A. 2009, Phys. Rev. D 80, 023524.
- Blanchet L. and Novak J., 2011, MNRAS 412, 2530.
- Burns J. O., Skillman S. W., O’Shea B. W., 2010, ApJ 721, 1105.
- Catinella B., Giovanelli R. and Haynes M. P., 2006, ApJ 640, 751.
- Cavaliere A. and Fusco-Femiano R., 1978, A&A 70, 677.
- Ciadullo R., Jacoby J. H., Djonghe H. B., 1993, ApJ 414, 454.
- Clowe D., Gonzalez A. & Markevitch M., 2004, ApJ 604, 596.
- Colín P., Klypin A., Valenzuela O. and Gottlöver S., 2004, ApJ 612, 50.
- Conroy C., Loeb A. and Spergel D. N., 2011, ApJ 741, 72.
- Davies P. C. W., 1975, J. Phys. A 8, 609.
- de Blok W. J. G. and Bosma A., 2002, A&A 385, 816.
- de Blok W. J. G., 2010, Advances in Astro. 2010, 789293.
- De Lorenzi F., Gerhard O., Saglia O. P., Sambhus N., Debattista V. P., Pannella M. and Méndez R. H., 2008, MNRAS 385, 1729.
- Deser S. and Levin O., 1997, Class. Quant. Grav. 14, L163.
- Diemand J., Zemp M., Moore B., Stadel J. ad Carollo M., 2005, MNRAS 364, 665.
- Doplicher S., Haag R. and Roberts J., 1971, Commun. Math. Phys. 23, 199.
- Doplicher S., Haag R. and Roberts J., 1974, Commun. Math. Phys. 35, 49.
- Dubinski J. and Carlberg R. G., 1991, ApJ 378, 496.
- Edmonds D., Farrah D., Ho C. M., Minic D., Ng Y. J. and Takeuchi T., 2014, ApJ 793, 41.
- Famaey B. and McGaugh S. S., 2012, Living Rev. Rel. 15, 10.
- Freidel L., Leigh R. G. and Minic D., 2014, Phys. Lett. B 730, 302.
- Freidel L., Leigh R. G. and Minic D., 2014, Int. J. Mod. Phys. D 23, no. 12, 1442006.
- Freidel L., Leigh R. G. and Minic D., 2015, JHEP 1506, 006.
- Frenk C. and White S., 2012, Annalen Phys. 524, 507.
- Govorkov A. B., 1983, Theor. Math. Phys. 54, 234.
- Greenberg O. W., 1990, Phys. Rev. Lett. 64, 705.
- Hawking S. W., 1975, Comm. Math. Phys. 43, 199.
- Ho C. M., Minic D. and Ng Y. J., 2010, Phys. Lett. B 693, 567.
- Ho C. M., Minic D. and Ng Y. J., 2011, Gen. Rel. Grav. 43, 2567.
- Ho C. M., Minic D. and Ng Y. J., 2012, Phys. Rev. D 85, 104033.
- Jacobson T., 1995, Phys. Rev. Lett. 75, 1260.
- Jacobson T., 1998, Class. Quant. Grav. 15, 251.
- Kaplinghat M. and Turner M. S., 2002, ApJ 569, L19.
- Klypin A., Kravtsov A. V., Bullock J. S. and Primack J. R., 2001, ApJ 554, 903.
- Mannheim P. D. and O’Brien J. G., 2013, J. Phys. Conf. Ser. 437, 012002.
- Mashchenko S. and Sills A., 2005, ApJ 619, 243.
- Mashchenko S. and Sills A., 2005, ApJ 619, 258.
- McGaugh, S. S., Schombert J. M., Bothun G. D. and de Blok W. J. G., 2000, ApJ 533, L99.
- McGaugh S. S., 2012, ApJ 143, no. 2, 40.
- Merrifield, M. R. 1992, AJ, 103, 1552
- Milgrom M., 1983, ApJ 270, 365.
- Milgrom M., 1983, ApJ 270, 371.
- Milgrom M., 1983, ApJ 270, 384.
- Milgrom M., 1999, Phys. Lett. A 253, 273.
- Moffat, J. W., & Rahvar, S. 2014, MNRAS, 441, 3724
- Moore B., Quinn T., Governato F., Stadel J. and Lake G., 1999, MNRAS 310, 1147.
- Moretti A., Gastaldello F., Ettori S. and Molendi S., 2011, A&A 528, A102.
- Navarro J. F., Frenk C. S., and White S. D. M., 1996, ApJ 462, 563.
- Navarro J. F., Frenk C. S., and White S. D. M., 1997, ApJ 490, 493.
- Norris M. A., Gebhardt K., Sharples R. M., Faifer F. R., Bridges T., Forbes D. A., Forte J. C., Zepf S. E., Beasley M. A., Hanes D. A., Proctor R. and Kannappan S. J., 2012, MNRAS 421, 1485.
- Penrose R., 1965, Phys. Rev. Lett. 14, 57.
- Persic M. and Salucci P., 1991, ApJ 368, 60.
- Persic M., Salucci P. and Stel F., 1996, MNRAS 281, 27.
- Romanowsky A. J., Douglas N. G., Arnaboldi M., Kuijken K., Merrifield M. R., Napolitano N. R., Capaccioli M. and Freeman K. C., 2003, Science 301, no. 5640, 1696.
- Rubin V. C. and Ford W. K. Jr., 1970, ApJ 159, 379.
- Rubin V. C., Ford W. K. Jr. and Thonnard N., 1978, ApJ 225, L107.
- Rubin V. C., Ford W. K. Jr. and Thonnard N., 1980, ApJ 238, 471.
- Sanders J. S. and Fabian A. C., 2002, MNRAS 331, 273.
- Sanders R. H., 1996, ApJ 473, 117.
- Sanders R. H., and Verheijen, M. A. W., 1998, ApJ 503, 97.
- Sanders R. H., 1999, ApJ 512, L23.
- Sanders R. H., 2003, MNRAS 342, 901.
- Sarazin C. L., 1988, “X-ray emissions from clusters of galaxies,” Cambridge University Press.
- Shevchenko V., 2008, Mod. Phys. Lett. A 24, 1425 [arXiv:0812.0185].
- Steinmetz M. and Navarro J. F., 1999, ApJ 513, 555.
- Susskind L., 1995, J. Math. Phys. 36, 6377.
- Swaters R. A., Sanders R. H. and McGaugh S. S., 2010, ApJ 718, 380.
- Taylor J. E. and Navarro J. F., 2001, ApJ 563, 483.
- Taylor M. A., Puzia T. H., Gomez M. and Woodley K. A., 2015 ApJ 805, 65.
- ’t Hooft G., 1993, Salamfest 1993, 0284 [arXiv:gr-qc/9310026].
- Tolman R. C., 1930, Phys. Rev. 35, 904.
- Tolman R. C. and Ehrenfest P., 1930, Phys. Rev. 36, 1791.
- Tully R. B. and Fisher J. R., 1977, A&A 54, 661.
- Torres-Flores S., Epinat B., Amram P., Plana H. and Mendes de Oliveira C., 2011, MNRAS 416, no. 3, 1936.
- Unruh W. G., 1976, Phys. Rev. D 14, 870.
- van Albada T. S., Bahcall J. N., Begeman K. and Sancisi R., 1985, ApJ 295, 305.
- van den Bosch F. C. and Dalcanton, J. J., 2000, arXiv:astro-ph/0007121.
- Verlinde E. P., 2011, JHEP 1104, 029.
- Vikhlinin A. Markevitch M., Murray S. S., Jones C., Forman W. and Van Speybroeck L., 2005, ApJ 628, 655.
- Vikhlinin A., Kravtsov A., Forman W., Jones C., Markevitch M., Murray S. S. and Van Speybroeck L., 2006, ApJ 640, 691 [Erratum: 2015, ApJ 799, 113].
- Zwicky F., 1933, Helvetica Physica Acta 6, 110.
- Zwicky F., 1937, ApJ 86, 217.

This paper has been typeset from a $\text{\TeX}/\text{\LaTeX}$ file prepared by the author.